Excitation energy transfer from the metastable excited He 2^3S_1 atom to the neon cryocrystal

1994 J. Phys.: Condens. Matter 6 2727

(http://iopscience.iop.org/0953-8984/6/14/010)

J. Phys.: Condens. Matter 6 (1994) 2727–2738. Printed in the UK

Excitation energy transfer from the metastable excited He 2^3S_1 atom to the neon cryocrystal

R A Zhitnikov and Yu A Dmitriev

A F Ioffe Physico-Technical Institute, 26 Politechnicheskaya Street, St Petersburg 194021, Russia

Received 8 July 1993, in final form 26 October 1993

Abstract. The effect of formation in a neon cryocrystal of atomic-type $2p^53s\ ^3P_2$ centres obtained as a result of He gas discharge products being trapped in a growing neon cryocrystal is discovered. The unstable excited $2p^53s^3P_2$ states in the neon cryocrystal were detected by ESR. This effect is interpreted as a new phenomenon: quasi-resonance transfer of excitation energy from the metastable He 2^3S_1 atom trapped in a growing neon cryocrystal to the exciton energy band of the neon crystal followed by the exciton self-trapping into the $2p^53p$ state and subsequent decay, ending in the $2p^53s^3P_2$ state recorded by ESR in our experiment. A temperature study showed that the rate constant λ of the process of excitation energy transfer from the He 2^3S_1 atom to the neon cryocrystal exciton band follows the Arrhenius-like law $\lambda - \lambda_0 \exp(-E/kT)$; the 'activation energy' E of the process turns out to be 0.0010(5) eV.

1. Introduction

An improved experimental set-up and technique described previously (Zhitnikov *et al* 1991, 1992) enabled us to observe by ESR unstable local excited states which form in rare-gas cryocrystals as gas discharge products are trapped in the growing cryocrystal. Using this technique the local unstable paramagnetic excited states in Ne, Ar, Kr and Xe cryocrystals were discovered and studied (Zhitnikov *et al* 1991, 1992). These states were interpreted as being metastable rare-gas $^3P_2$ atoms trapped from the gas discharge in a growing cryocrystal and become localized there in an anisotropic electric field of the surroundings distorted by the atoms.

Used here, the experimental set-up is similar to that described previously (Zhitnikov *et al* 1992). In the present study we have started a new set of investigations where, for the first time, pure He is passed through the gas discharge while pure Ne is fed to the substrate through a separate inlet tube, avoiding the gas discharge active part. A new effect has been found: the formation in a neon cryocrystal of local metastable excited states arising as helium gas discharge products are trapped in the growing neon cryocrystal.

2. Experimental procedure

The technique employed differs from the known methods as follows. The solid samples under studies are obtained by gas condensation on the thin-walled bottom of a quartz finger filled with liquid helium; the bottom of the quartz finger is used here as the substrate and is located at the centre of the microwave cavity of the ESR spectrometer. Both the He gas discharge and the matrix gas (Ne) flow passing through a separate inlet tube avoiding the

0953-8984/94/142727+12$19.50

gas discharge are cooled to liquid-nitrogen temperature. The products of the high-frequency gas discharge without intermediate feeding tubes are aimed in a vacuum directly onto the substrate, which prevents them from decay on the walls of the tubes. Thus, the sample is obtained directly in the cavity of the ESR spectrometer, which makes it possible not only to carry out ESR observation of the sample during the condensation but also to detect and study in the sample short-lived centres that are related to the gas discharge products.

The experimental set-up consists of a 3 cm ESR spectrometer with a microwave cavity cooled by liquid-nitrogen vapours, a gas filling and purification system, a high-frequency oscillator for exciting an electrodeless gas discharge, measuring instruments and pumping facilities.

Figure 1 shows the microwave cavity of the 3 cm ESR spectrometer, a low-temperature gas discharge device and the substrate cooled by liquid helium, on which the sample is condensed.

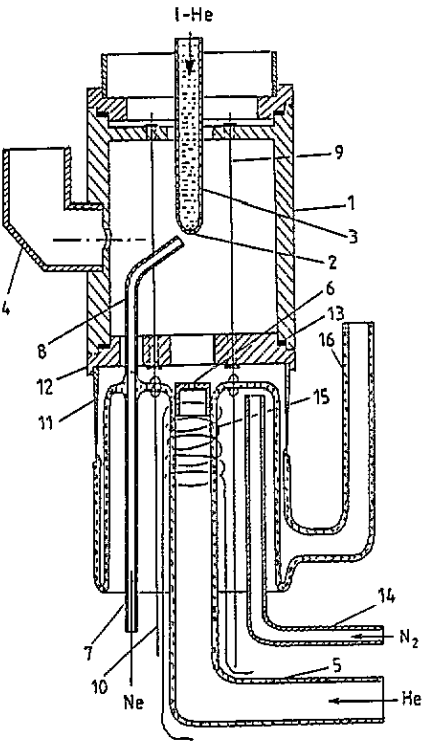

Figure 1. The main part of the experimental set-up including the microwave cavity of the ESR spectrometer, the gas discharge system, the gas inlet tube for matrix gas, and the quartz finger cooled by liquid helium (lHe) with the sample condensing on the bottom of the quartz finger as on a substrate (for notation see the text).

Here 1 is the cylindrical microwave cavity of the ESR spectrometer, 2 is the bottom of the quartz finger 3 filled with liquid helium, and 4 is a waveguide. The bottom 2 of the quartz finger is a low-temperature substrate for the gases being condensed. To improve the removal of the heat of condensation, the bottom of the quartz finger is made as thin as possible, 0.3–0.5 mm. An electrodeless high-frequency gas discharge is excited in the glass tube 5 with an outlet 6 of 0.2 mm diameter. The matrix gas could be supplied to the

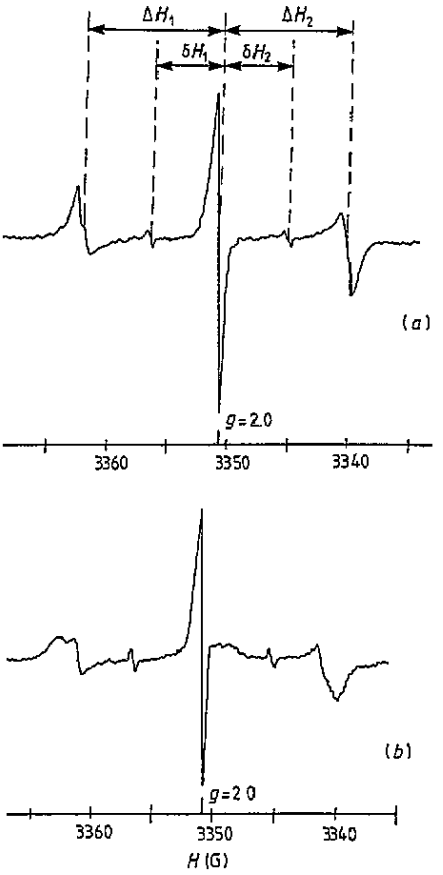

Figure 2. ESR spectra of unstable local excited states in a neon cryocrystal, which arise as a result of a He gas discharge product trapped in the growing neon cryocrystal. The magnetic resonance frequency f_{res} is 9381 MHz. The spectra in (*a*) and (*b*) were recorded without change in the experimental conditions.

substrate 2 by a glass tube 7 and further by a quartz tube 8 inserted into the cavity. The end of the quartz tube 8 is located close (3 mm) to the bottom 2 of the quartz finger, which facilitates effective freezing out of the matrix gas. Four rods 9 inserted into the cavity form two modulation loops. The magnetic field modulation current of the ESR spectrometer with a frequency of 100 kHz is taken to the rods through molybdenum wires 10 sealed into the glass. The glass part of the installation described above is sealed to a copper tube 11 which in turned is soldered to the cap 12. This cap is fastened to the microwave cavity by means of the indium gasket 13.

The whole device presented in figure 1 is cooled externally with liquid-nitrogen vapour and its temperature can be varied from 77 to 300 K.

A high-frequency (14 MHz) oscillator is used to maintain the discharge. The high-frequency power is fed through a coaxial cable to the coil 15 wound over the gas discharge tube 5. The oscillator can operate in either pulsed or continuous regime. The pulse duration can be decreased to 10^{-3} s, and the maximum pulse repetition rate is 30 kHz.

The glass tube 16 is used to measure the gas pressure in the cavity.

The experimental procedure is as follows. The pure He gas was passed through the liquid-nitrogen-vapour-cooled gas discharge tube 5, in which an electrodeless high-frequency pulsed discharge with a pulse duration of 3×10^{-5} s and a pulse repetition rate of 1–6 kHz was excited. Ground-state He atoms together with gas discharge products passed through the outlet 6 of the discharge tube 5 into the evacuated cavity and reached the bottom 2 of

the quartz finger 3 filled with liquid helium at 2.2–4.2 K. The pure Ne gas, also cooled by liquid-nitrogen vapour, was passed through the tubes 7–8, avoiding the gas discharge, onto the substrate, the Ne gas flow rate to the substrate being an order of magnitude above the He gas flow rate to the substrate. The ESR spectra of the sample were recorded continuously during its condensation, i.e. growth of the neon crystal with He gas discharge products trapped in the latter. The time constant of the recording system of the spectrometer, the field sweep rate and the frequency of the magnetic field modulation were 0.1 s, 0.2 G s^{-1} and 100 kHz, respectively.

The short-lived centres were separated from the stable centres by switching off the discharge, i.e. switching off the voltage on the coil 15 during recording the ESR spectrum.

We used high-purity rare gases with the following impurity contents: Ne 0.004% in, and He 0.01% in. Thus the impurity concentrations were sufficiently small to exclude their influence on the experimental results.

3. Experimental results

(i) The ESR spectra of the neon cryocrystal trapping the He gas discharge products are shown in figure 2. These spectra were observed during the neon condensation and disappeared at the instant when the discharge was turned off. On the other hand, no ESR spectra were observed in experiments where He flux was passed through the tube 5 with discharge running but with no Ne gas being fed onto the substrate through the inlet tubes 7–8. We found that the He gas discharge used cannot provide any ESR spectra before the Ne condensation as well as after the Ne flow is turned off despite a solid Ne layer condensed on the substrate 2 in a long-time run.

For simplicity we shall use the term 'edge-side lines' to denote the outer broad side lines in figure 2, and the term 'side lines' to refer to the inner narrow side lines.

The spectra shown in figures 2(*a*) and 2(*b*) were recorded under the same experimental conditions; so the differences in the edge-side lines are likely to be due to slight uncontrolled variations in these conditions.

There is absolute coincidence between both line positions and linewidths of the three middle lines in the He–Ne spectra (figures 2(*a*) and 2(*b*)) and the corresponding pure Ne lines monitored in our recent work (figures 2 in the papers by Zhitnikov *et al* 1991, 1992). Indeed, the g-factor and linewidth of the central line measured here appear to be 1.999 86(12) and 0.15(3) G respectively, and exactly the same as those for the pure Ne cryocrystal, 1.999 87(12) and 0.10(3) G. The side-line linewidths as well as separations between central and side lines are also the same; for pure Ne these are summarized in tables 1 in the above-cited papers. However, there is a significant difference between the spectra of the Ne cryocrystal obtained by condensation of the pure Ne passed through the discharge active part, and the spectra of solid Ne trapping He gas discharge products. The latter contains a pair of additional strong edge-side lines of unstable centres, located around the central line and separated from it by ΔH_1 and ΔH_2, for the high-field and low-field lines, respectively. These lines reveal the structure and each consists of at least two lines. The separation in magnetic field between each edge-side line and the central line is a factor of about 2 above the distances between each of the two weaker inner side lines and central line.

(ii) The fact that three middle lines of the He–Ne spectrum recorded here are clearly those of the pure Ne spectrum means that these spectra are due to centres of the same type and permits us to give an explanation of the nature of the He–Ne spectrum in the

same way as has been done previously for pure Ne (Zhitnikov *et al* 1991, 1992). This explanation is based on detailed analysis of the findings of experiments (Zhitnikov *et al* 1991, 1992) where the pure Ne fed through the tube 5 and gas discharge zone 15 (see figure 1) condenses together with the Ne gas discharge products on the substrate 2, and the second channel 7–8 is turned off, providing no gas flow through it; this is just the experiment with pure Ne. As noted above, the experiments with pure Ne yielded, in the neon cryocrystal, unstable paramagnetic centres whose spectra are identical in all their characteristics with that consisting of the three middle lines (central and two side lines) in figures 2(*a*) and 2(*b*) of the present paper. An explanation of the origin and character of these centres is as follows.

Charged particles leaving the gas discharge zone (electrons and ions) cannot be responsible for the formation of the unstable paramagnetic centres that we detected in Ne cryocrystals, because a strong (3300 G) magnetic field of the ESR spectrometer was turned on all the time during the experiments, thereby deflecting the particles (forcing them to follow small-radius trajectories) and completely preventing them from getting into the crystal. The light emitted by the Ne discharge is also not likely to be responsible for the effect, being capable of exciting only $^3P_1$ and $^1P_1$ states of Ne atoms whose very small radiative lifetimes should result only in very wide ESR lines, i.e. two to three orders of magnitude broader than observed lines. The most likely product of the gas discharge responsible for the ESR spectra observed is the metastable Ne $^3P_2$ atom trapped in the cryocrystal. This atom can reach the substrate because of its sufficiently long lifetime in the gaseous phase ($\tau_g = 20$ s) and causes narrow ESR lines to be observed in the experiments on account of its long lifetime in the cryocrystal ($\tau_c = 6 \times 10^{-4}$ s). Thus, it was concluded (Zhitnikov *et al* 1991) that the unstable paramagnetic centres observed in rare-gas solids are most probably provided by trapping in the growing crystal the metastable $^3P_2$ atoms of the same gas arriving at the substrate after being formed in the discharge.

Further it was noted by Zhitnikov *et al* (1991) that the above explanation of the origin of the spectra under study contains an essential difficulty related to the fact that all the centres observed yield only lines with g-factors close to 2 and located at a corresponding magnetic field of about 3300 G, while the $^3P_2$ state has $g = 1.5$ which would result in spectra situated at quite different fields around $H = 4400$ G. Check experiments revealed no lines in the vicinity of $H = 4400$ G. This was explained as follows. The rare-gas $^3P_2$ atom stabilized in a cryocrystal of this gas is presumably affected by the crystal electric field of sufficiently low symmetry (e.g. tetragonal). This field splits the $^3P_2$ term into two levels with $m_L = \pm 1$ and 0. If the splitting is sufficiently large, then at liquid-helium temperature (4.2–1.2 K) the lower $m_L = 0$ level with $g = 2$ is almost the only one to be populated. These atoms, making up the majority of the trapped $^3P_2$ atoms, seem to be responsible for the strong central line with $g = 1.999$.

The two side lines nearest to the central line of the spectrum in figure 2 can be explained as follows. If a $^3P_2$ atom is trapped in a position in the crystal where the effective crystal electric field has an axial symmetry component, its $m_L = 0$ state will split in zero magnetic field into two levels with $m_s = -1$ and $m_s = 0$, and therefore transitions $m_s = 0 \leftrightarrow m_s = +1$ and $m_s = 0 \leftrightarrow m_s = -1$ will move apart on the field scale, giving two lines equally distant from $g = 2$. The fraction of $^3P_2$ atoms trapped in a position with the crystal field of that kind is probably small and varies from run to run, which explains the change in intensity of the side lines.

One may suppose that most of the $^3P_2$ atoms are trapped in a substitutional site of a face-centred cubic (FCC) Ne crystal and give rise to the strong central line of the ESR spectrum (figures 2(*a*) and 2(*b*)), while the rest of the atoms, which vary from experiment

to experiment and are likely to depend on changes in experimental conditions hard to control, are trapped into octahedral interstitial sites of the crystal, providing the side lines.

It should be noted that the crystal electric field at these two trapping sites of an undistorted crystal is of very high (cubic) symmetry and therefore cannot cause splitting of the $^3P_2$ state. The low-symmetry (anisotropic) crystal field providing the observed ESR spectra with $g = 2$ is presumably due to lattice distortion caused by the s shell of this $np^5(n+1)s\,^3P_2$ atom. The FCC rare-gas lattice deformation and local rearrangement of this lattice by rare-gas P atoms have been considered elsewhere (Belov *et al* 1989). It was shown that the outward displacements of nearest lattice atoms can cause additional atoms to move into P-atom nearest surroundings, thereby breaking the lattice cubic symmetry and bringing a local low-symmetry electric field (e.g. tetragonal), including the axial component which affects the P atom. The dynamic Jahn–Teller effect can possibly also contribute in our experiments to the distortion of the cubic surroundings of the $^3P_2$ atoms trapped in the cryocrystal. Lattice defects, e.g. vacancies, can also account for the non-cubic surroundings of the $^3P_2$ atom.

Thus, the centres obtained in the present work can be interpreted as being atomic-type excited $2p^53s\,^3P_2$ states which become localized in the FCC Ne crystal lattice, shift the nearest matrix atoms outwards, rearrange their surroundings and are subjected to the action of the anisotropic electric field of this environment which, being rearranged, is no longer of cubic symmetry.

The nature of the strong edge-side lines which occur only when a neon cryocrystal is trapping the He gas discharge products will be discussed in the following. We believe that these are also related to the $2p^53s\,^3P_2$ centres, but with the surroundings distorted in a different way.

(iii) While the nature of the neon cryocrystal excited states recorded here is believed to be clear, the mechanism of their production is to be determined. Indeed, in the experiments on pure rare gases (Zhitnikov *et al* 1991, 1992), the excited Ne $^3P_2$ atoms (as well as Ar, Kr and Xe atoms), which are trapped in the growing cryocrystal and rearrange the nearby crystal lattice, form directly in the gas discharge, whereas in the present study the gas flows aimed onto the substrate contain no excited Ne atoms at all, including $^3P_2$ atoms. Apart from ground-state He atoms, the only incoming He gas discharge products at the growing Ne cryocrystal are the metastable He 2^3S_1 and 2^1S_0 atoms. Other excited helium atoms have too short lifetimes to reach the substrate from the gas discharge. Charged particles from the discharge can also be excluded from consideration, since they are deflected from the substrate by the strong magnetic field of the ESR spectrometer (Zhitnikov *et al* 1991, 1992).

Thus, the atomic-type excited $^3P_2$ states of the neon cryocrystal which are observed here originate from the excitation energy of incoming metastable He atoms from the gas discharge.

Special experiments were carried out in which pure He was passed through the discharge tube 5 while pure gaseous Ar or Kr, instead of Ne, was fed to the substrate through the inlet tube 7–8, avoiding the gas discharge active part. No ESR spectra were observed in these He–Ar and He–Kr pulsed-discharge experiments, while very weak signals were recorded with strong continuous He discharge. This is undoubtedly an important result, for it means that the energy transfer from the metastable excited He atoms to the neon sample is unique, i.e. this is a resonance or quasi-resonance process which is due to some features of the relative positions of the Ne and metastable atomic He energy levels. Indeed, it is well known that there is close coincidence between the He 2^3S_1 and the Ne $2p^54s$ states, as well as between the He 2^1S_0 and Ne $2p^55s$ states, which is used in the helium–neon laser

to transfer excitation energy from He to Ne atoms. As for the Ar and Kr atoms, all their levels lie far below the lowest excited He level, and therefore the excitation energy cannot be exchanged between the metastable He atom and Ar or Kr atoms. The weak ESR signals observed in the He–Ar and He–Kr experiments with strong continuous He discharge are likely to be due to ionization of these atoms with metastable excited He atoms that cannot ionize Ne atoms. This effect is at present being investigated.

It has been shown by Jones *et al* (1969) that the energy transfer from the metastable He 2^3S_1 and 2^1S_0 atoms to Ne atoms is a quasi-resonance process and the reaction rate constants obey the Arrhenius law $K(T) = K_0 \exp(-E/kT)$, where K is the reaction rate constant, T the absolute temperature and E the 'activation energy' of the process. In the above paper it is found that $E = 0.051$ eV for the energy transfer from He 2^3S_1 to Ne, and $E = 0.041$ eV for the energy transfer from He 2^1S_0 to Ne. The former value is close to the defect of resonance of the excitation energy transfer process from He 2^3S_1 to Ne $2p^54s$, i.e. to the difference between the He 2^3S_1 and Ne $2p^54s$ excitation energies while the latter is close to the defect of resonance of the energy transfer process from He 2^1S_0 to Ne $2p^55s$.

(iv) On the assumption that the above quasi-resonance process of excitation energy transfer from the metastable He 2^3S_1 and 2^1S_0 atoms to the ground-state Ne atom occurs in our experiments, it may be expected then that the Ne $2p^54s$ and $2p^55s$ atom states decay by a fast radiation cascade to the lowest metastable $2p^53s\,^3P_2$ state, the state which becomes localized in a neon cryocrystal, rearranging its surroundings. In that case the temperature dependence of the $^3P_2$-centre production or the temperature dependence of the ESR signal intensity (figure 2) should also be exponential or obey an Arrhenius law.

Consider the production and decay kinetics of the $^3P_2$ centres observed here by ESR. Let $N_1 = N$ (Ne $^3P_2$) be the number of $^3P_2$ centres localized in the sample giving the ESR signal observed. Hence N_1 is proportional to A, the ESR signal intensity. If N_2 represents the number of metastable He atoms per second which, on reaching the sample, transfer their excitation energy to it, then $dN_1/dt = \lambda N_2 - (1/\tau)N_1$, where λ is the rate constant of the excitation energy transfer from the metastable He atom to the Ne atom, τ is the lifetime of the $2p^53s\,^3P_2$ state in the neon cryocrystal. In a steady state, which is the case in our experiments, $dN_1/dt = 0$, and hence $N_1 = \lambda\tau N_2$, N_2 being constant.

We found experimentally that, at constant N_2, N_1 depends upon temperature, which means that the product $\lambda\tau$ is a function of temperature: $\lambda\tau = a = a(T)$, and $N_1(T) = a(T)N_2$. Our experiments show a decrease in the ESR signal amplitude, and therefore in N_1 and hence $\lambda\tau$, with decreasing temperature.

It was then supposed that, as in the case of atomic collisions in a gas, the Arrhenius law applies to the rate constant of the excitation energy transfer from the metastable He atom to the Ne atom occurring in our experiments, i.e. $\lambda = \lambda_0 \exp(-E/kT)$. Moreover, the lifetime τ of the Ne $^3P_2$ atom in the neon cryocrystal was assumed to be independent of temperature. These assumptions lead us to suppose that the ESR signal intensity also obeys the Arrhenius law $N_1 = N_{10} \exp(-E/kT)$. Further experiments described below have been carried out in order to verify the assumptions.

Since it is very difficult to determine experimentally the flow of metastable He atoms, i.e. the value of N_2 and the coefficient λ_0, the quantity $N_{10} = \lambda_0\tau N_2$ is unknown. To exclude this from consideration, we shall deal with the ratio $N_1(T_2)/N_1(T_1)$, where T_1 is the starting temperature, usually 4.2 K, and T_2 varies in the range from 4.2 to 2.2 K. For this ratio, it is reasonable to expect the following dependence on T_1 and T_2:

$$N_1(T_2)/N_1(T_1) = \exp[-(E/k)(1/T_2 - 1/T_1)].$$

Based on the experimental data the ratio $N_1(T_2)/N_1(T_1)$ was plotted against $1/T_1 - 1/T_2$ in order to clarify whether the Arrhenius law $N_1(T_2)/N_1(T_1) = \exp[-(E/k)(1/T_2 - 1/T_1)]$ holds in this case.

(v) Line A in figure 3 shows a plot of $\ln[N_1(T_2)/N_1(T_1)]$ as a function of $1/T_1 - 1/T_2$. In our experiments, the substrate temperature or, correspondingly, the temperature of the sample growing on the substrate 2 (figure 1) is lowered by the pumping of liquid-helium vapour. The sample temperature is detected by measuring the gas pressure in the liquid-helium bath.

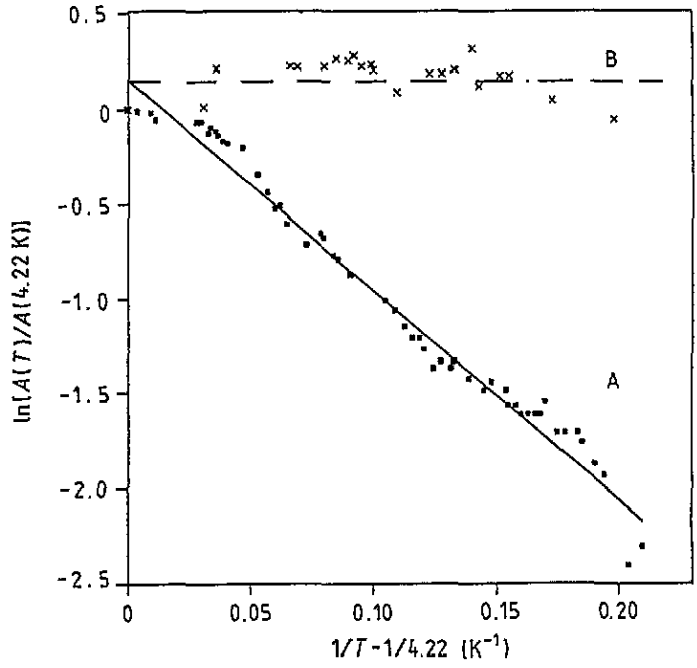

Figure 3. The temperature dependence (line A) of the signal amplitude $A(T) \sim N_1(T)$ obtained for the central line of the spectrum in figure 2 of the present paper. The dependence is given in a temperature range from 2.2 to 4.22 K. The slope of line A is related to the 'activation energy' of $E = 12.1$ K $\simeq 0.001$ eV. The temperature dependence (line B) for the central line (see figures 2 in the work of Zhitnikov *et al* (1991, 1992)) of the ESR spectrum yielded by $^3P_2$ neon atoms trapped in the neon cryocrystal from the neon gas discharge is also shown.

It can be seen from figure 3, line B, that the experimental dependence $\ln[N_1(T_2)/N_1(T_1)]$ as a function of $1/T_2 - 1/T_1$ can be fairly well approximated by a straight line whose slope gives us the value of the 'activation energy': $E \simeq 12$ K $\simeq 0.001$ eV. Using either increasing or decreasing sample temperature, we have recorded many such experimental dependences in the temperature range 2.2–4.2 K. If we take into account the statistical scattering of the experimental data, the 'activation energy' can be estimated as $E = 12(6)$ K $= 0.0010(5)$ eV.

To support the idea that λ does depend exponentially on temperature with the 'activation energy' estimated above, one has to verify that the lifetime τ of the $2p^5 3s\,^3P_2$ state in the neon cryocrystal is independent of temperature. The radio-frequency saturation of the central line (figure 2) has been used to accomplish this. Saturation measurements similar to those described in the previous paper in detail (Zhitnikov *et al* 1992) enabled us to observe an

effective time T_1^*. It is shown in the above paper that T_1^* is a low limit of the lifetime τ of the unstable paramagnetic $^3P_2$ centre, i.e. $\tau > T_1^*$, where $T_1^* = \tau T_1/(\tau + T_1)$, and T_1 is the $^3P_2$ centre spin–lattice relaxation time (Zhitnikov *et al* 1992).

The experiments indicate that T_1^* varies with temperature or, more specifically, decreases with decreasing temperature. This means that either the lifetime τ or the relaxation time T_1 (or both these quantities) depends on temperature. To clarify this, particular experiments were carried out in which temperature dependence of $^3P_2$ ESR signal amplitude was recorded for the neon cryocrystal, with pure Ne passing through the gas discharge active part, tube 5. This procedure is similar to that used earlier (Zhitnikov *et al* 1991, 1992). Other gases, including helium, were not used in these experiments. We have found (see figure 3, line B) that the ESR signal intensity or the number of $^3P_2$ centres is independent of temperature in the whole range 2.2–4.2 K; this result means that the $2p^53s\,^3P_2$ centre lifetime τ in the neon cryocrystal does not depend on temperature. Since the nature of the neon cryocrystal $^3P_2$ centres produced by the trapping of metastable helium atoms in solid neon is exactly the same as that of the centres obtained by the neon gas discharge, the lifetime τ is certainly also independent of temperature for the former method of production. For the latter method, we have also found T_1^* to vary with temperature. Since τ does not depend on temperature, the temperature dependence of T_1 is apparently the only factor contributing to the temperature dependence of the relaxation time T_1^*. Moreover, the temperature dependences of T_1^* measured in both neon discharge and helium discharge experiments turned out to be the same. This is further strong evidence for the above conclusion that the T_1^* temperature dependence originates exactly from the T_1 temperature dependence while the lifetime τ of $^3P_2$ centres in the neon cryocrystal is independent of temperature.

Based on the above conclusion, the temperature dependence of the product $\lambda\tau$ comes entirely from that of λ, the rate constant of the energy transfer from the metastable He atom to the neon cryocrystal, which has the form, according to the experimental results given in figure 3, line B, $\lambda = \lambda_0 \exp(-E/kT)$, the 'activation energy' being $E = 12(6)$ K $= 0.0010(5)$ eV.

4. Interpretation

The experiments that we have just described show that the 'activation energy' of the process of the energy transfer from the metastable excited He atom to the Ne cryocrystal, which appears to be $E = 0.0010(5)$ eV, is a fortieth to a fiftieth of the 'activation energies' of 0.0051 and 0.0041 eV reported by Jones *et al* (1969) for the energy transfer from the metastable He 2^3S_1 and 2^1S_0 atoms, respectively, to the free neon atom. Thus, this indicates that the effect found in our experiments cannot be explained on the basis of the process of excitation energy transfer from the metastable He atom to the ground-state Ne atom. To explain the excitation energy transfer from the metastable He atom to neon cryocrystal, one has obviously to search for an entirely different process.

The effect that we have found may be interpreted as follows.

From many optical investigations the schematic diagram of neon cryocrystal energy levels, bands and transitions is well known, and this is presented in figure 4 according to the work by Belov *et al* (1989).

Shown in this figure is the exciton band discovered by Inoue *et al* (1984) (and later given the name of the 'X-exciton' band) in investigations of excitation spectra of the visible luminescence corresponding to $2p^53p$–$2p^53s$ ($3p_i$–$3s_k$ in figure 4) transitions.

Our explanation of the effect found in the present work is as follows.

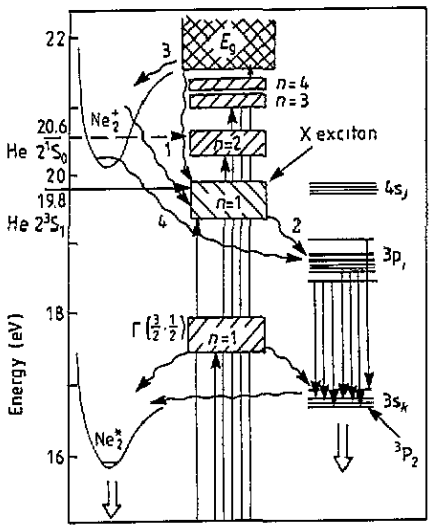

Figure 4. Schematic diagram of the energy levels, bands and transitions for the excited states of the neon cryocrystal. The energy levels of the metastable He 2^3S_1 (19.82 eV) and 2^1S_0 (20.62 eV) atoms are indicated, and the ways in which these excitation energies can be quasi-resonantly transferred to the neon cryocrystal bands are shown.

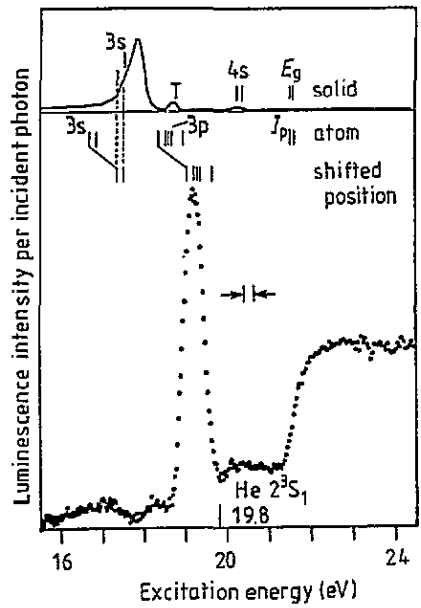

Figure 5. Excitation spectrum of the visible luminescence. The upper part of the figure shows the reflectance spectrum, where the vertical bars indicate the relevant levels of the exciton and the free atom: E_g, band gap; I_p, ionization energy; T, structure identified as due to reflection from the substrate.

We have added energy levels of the metastable He 2^3S_1 (19.82 eV) and 2^1S_0 (20.62 eV) atoms to the schematic diagram in figure 4. It can be seen from this figure that the energy level of the He 2^3S_1 atom appears to be located near the top of the X-exciton energy band. This permits us to suppose that there exists an effective energy transfer from the metastable He 2^3S_1 atom to the neon cryocrystal X-exciton band. We believe that the most probable way of producing $2p^53s(3s_k)\,^3P_2$ atomic states in the neon cryocrystal is the quasi-resonance excitation energy transfer from the metastable He 2^3S_1 atom to the neon cryocrystal X-exciton band followed by the self-trapping of the exciton into the $2p^53p$ ($3p_i$ in figure 4) ten-level state (path 2 in figure 4) which then decays to the lower $2p^53s$ four-level excited state ($3s_k$ in figure 4) whose lowest $^3P_2$ level is just that observed in our experiment. It is well known from the optical investigations that the self-trapped X-exciton is actually the $2p^53p$ atomic-type state decaying to the $2p^53s$ state with luminescence in the visible region.

The excitation energy (19.82 eV) transfer from the He 2^3S_1 atom to the neon cryocrystal X-exciton band should be a quasi-resonance process, since the centre of the band shown in figure 5 originated from the paper of Inoue *et al* (1984) is at 19.2 eV while the band half-width is about 0.6 eV. Thus, the energy transfer from the He 2^3S_1 atom is not of a completely resonant nature. The fact that the 'activation energy', i.e. the 'defect of resonance', of the energy transfer process is so small ($E = 0.001$ eV) can be explained as being due to the broad wings of the exciton band (figure 5). The temperature dependence of the probability of such an energy transfer seems likely to be determined by the neon cryocrystal phonon spectrum and the shape of the high-energy wing of the band shown in figure 5 in the region

close to 19.8 eV.

The above mechanism of production of the Ne $2p^5 3s\,^3P_2$ centres, which explains their existence as being the result of trapping of the metastable He 2^3S_1 atoms in the growing neon cryocrystal, enables us to explain the additional edge-side lines separated by ΔH_1 and ΔH_2 from the central line in the ESR spectra of the $^3P_2$ centres shown in figure 2. The nature of these lines is presumably similar to that of the weak side lines centred around the central line at the distances δH_1 and δH_2, which has already been discussed (Zhitnikov *et al* 1991, 1992). Each of these pairs of lines possibly results from the influence of an axially symmetric anisotropic crystalline electric field on the $^3P_2$ atomic-type centre, which is due to the outward shift, the distortion and the rearrangement of the $^3P_2$ centre nearest surroundings in the neon cryocrystal (Zhitnikov *et al* 1991, 1992). When a $^3P_2$ atom is trapped in the neon cryocrystal directly from the neon discharge, as it has a large radius, it causes the neighbouring matrix atoms to shift outwards, thus producing a rearrangement of its nearest surroundings. This is the reason why the axial field occurs, which gives rise to the weak side lines displaced from the central line by δH_1 and δH_2. On the other hand, when metastable He atoms are trapped in the neon cryocrystal there may be additional deformation of the lattice in the vicinity of the Ne $^3P_2$ atoms which are produced according to the mechanism described earlier in this paper. This deformation can be provided by the energy produced during X-exciton self-trapping and by the fact that the radius of the $2p^5 3p$ state, which is intermediate in the process of $2p^5 3s\,^3P_2$-state formation in the neon cryocrystal, is even larger than that of the $^3P_2$ atom. This additional lattice deformation occurring around some of the Ne $^3P_2$ atoms gives rise to new paramagnetic $^3P_2$ centres yielding the strong edge-side lines centred around the central line at the distances ΔH_1 and ΔH_2 from this (figure 2). Centres arising under these lattice distortions may be of several types, depending on the different metastable configurations generated at the nearest surroundings of the $3p^5 3s\,^3P_2$ state. It is these centres of several types that produce those unresolved components comprising edge-side lines in figure 2, the distinctions between the spectra in figures 2(*a*) and 2(*b*) being the result of the variations in type and number in the centres which are hard to control from run to run. Certain of the components of the edge-side lines may be somewhat anisotropic, which can also lead to changes in the edge-side lines, for a polycrystalline sample. It should be noted that the two types of paramagnetic centre yielding the central and two nearest side lines are isotropic, to judge from the high symmetry and small width of these lines (figures 2(*a*) and 2(*b*)).

The process of lattice deformation and defect production in the neon cryocrystal during exciton self-trapping into the atomic-type state has been investigated by Savchenko *et al* (1988).

To conclude, the following may be noted.

It can be seen from figure 4 that the energy level of the second metastable He atom, 2^1S_0, hich also may be trapped in the neon cryocrystal, is close to the top of the other exciton band with $n = 2$. This probably gives the possibility of quasi-resonance transition of the excitation energy from the He 2^1S_0 atom to the neon cryocrystal. However, it is difficult to draw any conclusion at the present time about whether this process actually occurs and whether the $2p^5 3s\,^3P_2$ atomic-type state will be generated.

References

Belov A G, Svishchev V N and Fugol' I Ya 1989 *Fiz. Nizk. Temp.* **15** 61–71
Inoue K, Sakamoto H and Kanzaki H 1984 *Solid State Commun.* **49** 191–3
Jones C R, Niles F E and Robertson W W 1969 *J. Appl. Phys.* **40** 3967–9

Savchenko E V, Rybalko Yu I and Fugol' I Ya 1988 *Fiz. Nizk. Temp.* **14** 399-412
Zhitnikov R A, Dmitriev Yu A and Kaimakov M E 1991 *Sov. Phys.–JETP* **72** 1009–15
Zhitnikov R A, Dmitriev Yu A and Kaimakov M E 1992 *Sov. J. Low Temp. Phys.* **18** 532–8